T.V. Tkachenko, D.S. Kamenskyh, Y.V. Sheludko, V.O. Yevdokymenko

STRUCTURAL AND MORPHOLOGICAL FEATURES OF MICROCRYSTALLINE CELLULOSE FROM SOYBEAN STRAW BY ORGANOSOLVENT TREATMENT

V.P. Kukhar Institute of Bioorganic Chemistry and Petrochemistry of National Academy of Sciences of Ukraine
1 Murmanskaya Str, Kyiv, 02094, Ukraine, E-mail: ttv13ttv@gmail.com

The main idea of this work is to study the possibility of obtaining microcrystalline cellulose from multi-ton and low-value agricultural waste and investigation its structural properties. Air-dry soybean straw, an agricultural waste, was used for the research. Microcrystalline cellulose (MCC) was obtained from it by the method of organosolvent cooking. Using the methods of XRD, XRF, FTIR-ATR, AFM, TGA and DSC, the structure and morphology of MCC were studied. It is found that increasing the hydromodule reduces the content of lignin and inorganic components. At the same time, both the yields of the MCC and its qualitative characteristics are declining. First of all, the crystallinity index of the MCC decreases with the increasing amount of the liquor ration. The band corresponded to symmetric CH_2 bendings at 1435–1429 cm^{-1}, that is known as the crystallinity band, decreased with increasing amount of the liquor ration. The AFM method shows that when forming the surfaces of MCC 10 particles, not only groups of particles are formed, the heights of the elements of which range from 23.8–28.1 to 16.9–26.8 nm, but also elongated units on the surface of which there are individual particles. The surface roughness is 1.6 nm. At the same time, the surface of the MCC 15 has a surface roughness Ra = 3.1 nm. The particles are distributed throughout the scan, with no clusters of particles and their agglomerates, and their heights are 14.4; 18.7; 20.6; 17.4 and 23.9; 18.1; 24.7 nm. 3D image of the particles showed that the particles are pyramids of different configurations similar to the particles in the MCC 10. It should be noted that the range of depressions and heights characteristic of MCC 15 is much smaller (from –13 to +20.7 nm) than in the MCC 10 (from –17.5 to 45.5 nm).

*Keywords: microcrystalline cellulose, soybean straw, liquor ration, relief of the surface, atomic force microscopy*

INTRODUCTION

For the first time in the '50s of the twentieth century, Battista introduced the term "microcrystalline cellulose" (MCC) and "degree of polymerization of cellulose" (DP). They studied it in detail and proposed a scheme for the destruction of the amorphous components in lignocellulosic biomass. In 1955 Battista and Smith first commercialized it under the Avicel brand [1]. In 1964, FMC introduced Avicel pH in the pharmaceutical industry as an ingredient for direct compression tablets [2]. MCC was first registered in the supplement market in 1966 in the 12th edition of Natural Formulary [3]. MCC has a powdery morphology and consists of particles that are aggregates of microcrystallites of cellulose, destructed to the so-called "limit" degree of polymerization. Dependent on the source of cellulosic material and the conditions of production, the average particle sizes of different types of MCC are in the range from 1 to 400 μm. Their characteristic feature is a

significant violation of the fibrillar structure of surface fibres, associated with the violation of individual elements of the fibres of the original cellulose (amorphous layers), which play the role of connections between fibrils (Fig. 1) [4]. The xylem of herbaceous plants is much easier to physically and chemically process than wood of coniferous and deciduous species. This can be explained by the following reasons. Coniferous wood has a relatively simple structure, as 90–95 % consists of tracheids – long thin cells with flat or spindle-shaped closed ends. Thick-walled late tracheids provide mechanical strength. In deciduous wood, the main mechanical tissue consists of libriform fibres and fibrous tracheids. The main anatomical elements of herbaceous plants are fibres then blood vessels, parenchymal and epithelial cells. The density of the xylem is determined by the number and diameter of vessels, the number of parenchymal cells, as well as the wall thickness of libriform fibres or tracheids. Due to the

anatomical structure of the xylem, the greater density of the cells that form it, and less lignification, herbaceous plants are easily exposed to physicochemical effects. Thus, the anatomical and chemical structure of herbaceous plants explains their easier physico-chemical

processing compared to wood [5–17]. Ukraine is a country with developed agriculture, produces a large number of grain and industrial crops, the processing of which annually produces a significant number of by-products of fibrous products that can be used for pulp production.
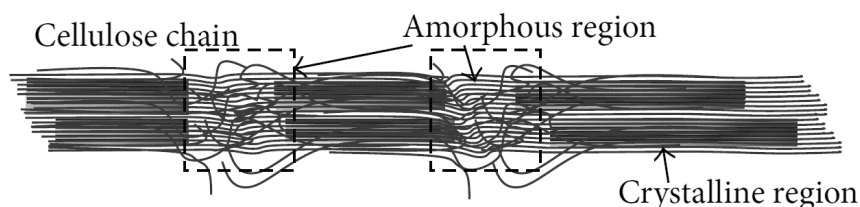
Fig. 1. Components of cellulose [4]

Hydrolysis cooking is proposed to be used as the second stage in obtaining MCC [18–20]. The most common is the organosolvent method – the use of a mixture of acetic acid and hydrogen peroxide in different ratios [18–20]. Other solutions of acids in different concentrations are also used [21–23]. The result is obtainig of MCC and/or nanocellulose.

At the same time, the literature does not contain enough information about the effect of different ratios of pulp over liquor (hydromodule) on the physicochemical characteristics of MCC from non-wood raw materials.

MATERIALS AND METHODS

Air-dry soybean straw, an agricultural waste, (fraction 2–5 mm) from Kyiv region of Ukraine with the following characteristics: humidity 8 %, the proportion of organic components to dry weight of 95.6 % (cellulose – 46.9, hemicellulose – 36.3, lignin – 11.6 mass. %) and the proportion of inorganic components – 4.4 % was used. The chemical composition of flax ash (inorganic components) determined by using XRF are shown in Table 1.

Table 1. Composition of initial soybean straw ash

Elements	Content mass.%
O	25.044±0.206
Si	2.451±0.083
P	0.187±0.043
S	0.769±0.022
Cl	2.603±0.045
K	32.786±0.176
Ca	34.849±0.187
Fe	0.180±0.004
Mn	0.078±0.004
Sr	0.132±0.01
Ti	1.033±0.011

MCC was obtained from soybean straw by the method of organ-solvent cooking described in [24]. Soybean straw was hydrolysed with the solution CH_3COOH-H_2O_2-H_2SO_4-H_2O at 105 °C for 3 hours with constant agitation in the liquor ratio of 10 (MCC 10) or 15 (MCC 15) (hydromodule). The reaction mixture was then

filtered at room temperature and washed repeatedly with distilled water to neutral pH. It was oven-dried at 105 °C for 8 h. The cellulose yield (Y) was calculated using Equation (1).

$$Y = \frac{m_1}{m_2} \times 100\% , \tag{1}$$

where m_1 – absolute weight of cellolose after treatment and m_2 – absolute weight of cellolose befor treatment.

The contents of cellulose, hemicellulose, lignin and other chemical components in cellulosic products were determined by standard chemical analysis, described earlier [25]. All chemical analysis was carried out twice allowing calculating the mean values and standard deviations, which do not exceed 5 %. The inorganic components were determined using Expert 3L XRF (INAM, Ukraine). The degree of polymerization (DP) of cellulose samples was determined by viscosity measurements in a cadmium ethylenediamine solution using an Ostwald viscometer [26]. The phase identification of the products was examined under X-ray diffraction (XRD) using a MiniFlex 300/600 diffractometer (Rigaku, Japan). The diffraction patterns were recorded using CuK_α radiation ($\lambda = 0.15418$ nm), the operating voltage of 40 kV and a current of 15 mA. XRD pattern of samples was obtained in the 2θ range between 10º and 60º with a step of 0.02º. The crystallinity index (CI) [27] was calculated according to Eq. (2).

$$CI = \frac{I_{22}}{I_{22} + I_{18}} \times 100\% \ , \qquad (2)$$

where I_{22} and I_{18} are the crystalline and amorphous intensities at 2θ scale close to 22 and 18°, respectively. FTIR analysis of the obtained cellulose was performed using an IRAffinity-1S FTIR spectrometer (Shimadzu, Japan) equipped with a Quest ATR Diamond GS-10800X (Specac, UK) within the wavenumber range of

4000 to 400 cm^{-1}. The surface morphology was investigated with atomic force microscope (AFM) NT-206 (Company with double liability "Microtestmachines", Belarus) equipped with standard sonde CSC37 and rigidity of console 0.3–0.6 N/m. The scan was run in a contact static mode at 10 mcm/s with a step of 0.3 nm. Samples of cellulose (4 mg) after grinding for 1, 2 and 5 min were stirred in ethyl alcohol (5 ml) for 15 min. The resulting suspension (0.25 ml) was applied to quartz glass and dried at 50 °C to constant weight. Then the scan was performed on AFM. Thermogravimetric analysis (TGA) and differential scanning calorimetric analysis (DSC) were performed with a PT1600 TG-DTA/DSC (STA Simultaneous Thermal Analysis, LINSEIS Messgeräte GmbH, Germany). The samples (13.0±0.1 mg) were collected in a standard corundum pan. The scan was run at 5 °C/min under a flow of air. The mass change was measured from 15.8 to 1000 °C. The sample was analysed three times.

RESULTS AND DISCUSSION

A white, tasteless and odorless MCC was obtained under the earlier described method from soybean straw. The MCC's percentage yield was calculated by Eq. 1 (Table 2). The results of the chemical composition of obtained MCC were determined using the above-described methods and the data were summarised in Table 2. It was found that increasing the liquor ration from 10 to 15 has no significant effect on the yield of cellulose products and cellulose content.

**Table 2.** The main characteristics of obtaining MCC from soybean straw

Liquor ration	Cellulose yield (Y), %mass.	Ash, %mass.	Cellulose, %mass.	Klason lignin, %mass.	CI, %	DP
10	99.8	0.8	96.6	3.4	0.70	275
15	97.5	0.5	97.8	2.2	0.67	384

The X-ray diffraction (XRD) patterns of the MCC from soybean straw under different cooking conditions are presented in Fig. 2. On the diffraction patterns of cellulose samples (Fig. 2) the peaks were observed at: 14–16 °; 22–23 °; 34–35 °, relating to the reflection of the planes 10-1, 101; 002; 040 cellulose crystal lattice, respectively. Peaks in the region

2θ = 15–16 ° are associated with the diffraction of X-rays from the planes 10-1 and 101 of the crystal lattice of cellulose I. The intensity of the peak reflex in the region 2θ = 22–23 ° corresponds to the plane 002 of the crystal lattice of natural cellulose I [24, 28]. profile of amorphous cellulose scattering has a characteristic diffusion character with a

maximum of 2θ = 18.5–19 °. However, as can be seen from the above diffractograms, cellulose obtained in cooking solution with a larger liquor ration is characterized by a more amorphous structure, which is typical for MCC obtained under such conditions from other lignocellulosic biomass (Fig. 2 *b*). This is also confirmed by the values of the crystallinity index and the degree of polymerization (Table 2). It can be seen that the CI of MCC 15 (Table 2) decreased with an increase in liquor ration, confirming that it had a notable effect on the deformation of crystal structure and fragmentation of crystalline grains. After such treatment, the initial packing of polymer macromolecules was changed [28, 29]. It can be seen (Table 2) that the DP of MCC increased with an increase in liquor ration, indicating an increase in the number of d-anhydro glucopyranose units in cellulose molecules.
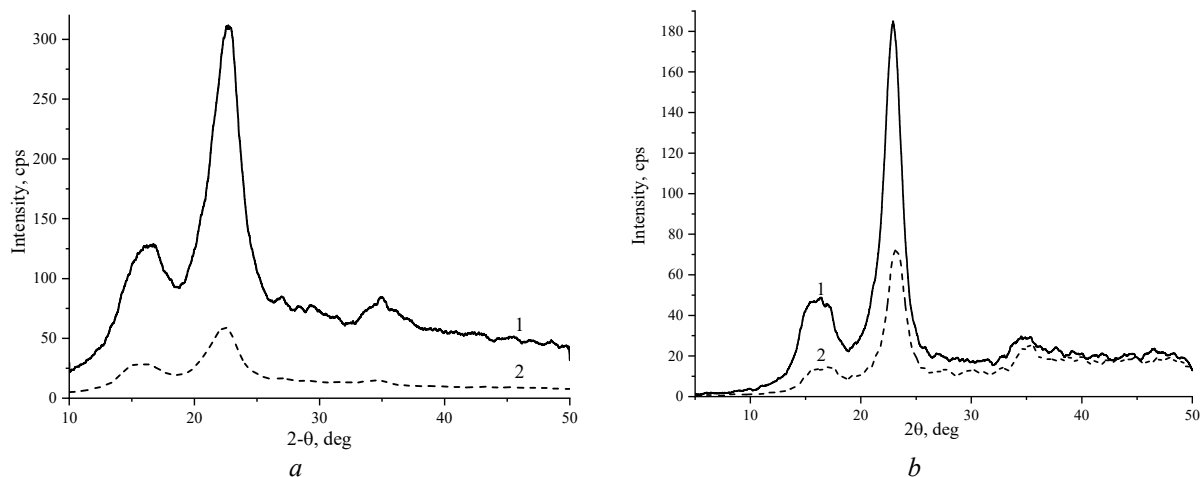
Fig. 2. XRD patterns of MCC obtaining from soybean straw (*a*) and flax (*b*) at different liquor ration: *1* – 10, *2* – 15

Fig. 3 demonstrates the FTIR-ATR spectra of the obtained MCCs compared to the industrial design. All samples display two main absorbance regions. These regions are found at high wavenumbers 2800–3500 cm^{-1} and low wavenumbers 500–1700 cm^{-1}, respectively. In general, microcrystalline cellulose samples showed a strong and wide band at 3381–3335 cm^{-1}, which belong to stretching vibration of –OH group. The characteristic peak at 2915–2900 cm^{-1} was because of the symmetric C–H vibrations. The peak at 1740–1720 cm^{-1} in the obtained MCC corresponds to the acetyl and uronic ester groups of the hemicelluloses or the ester linkage of the carboxylic group of the ferulic and *p*-coumeric acids of lignin and/or hemicelluloses [30, 31]. This agrees well with the data in the Table 2. Strong absorption at 1645–1635 cm^{-1}) belonged to adsorbed water a cellulose surface. Moreover, the peaks at 1076–1060, 899–897 and 1119–1116 cm^{-1} referred to the stretching vibration of C–O, C–OH out of plane bending mode [32] and stretching vibration intermolecular ester bonding. Absorption bands in the field 899–668 cm^{-1} can be carried both to the pulsation vibrations of a piranoze ring, and deformation vibrations of C–H. The band in the absorption region at 900 cm^{-1} characterizes the asymmetric vibrations in antiphase and the vibrations of the C1 atom and the four surrounding atoms of β-glycosidic structures. This band is called the amorphous band [33]. Distinct bands in the fields 2915–2900 and 1435–1429 cm^{-1} testify to that the sample is characterized by the high degree of the orderliness of macromolecules. The band corresponding to symmetric CH$_2$ bendings at 1435–1429 cm^{-1} decreased ground MCC as compared unground MCC. This band is known as the crystallinity band, where the increase in the intensity demonstrates a higher degree of crystallinity [34]. Splitting of a band of absorption of deformation vibrations of OH–groups at 1380–1370 cm^{-1} also can testify to removal at the hydrolysis of fragments of cellulose connected by weak hydrogen bond and inclusion remained OH–groups in stronger intermolecular hydrogen bond [35]. In other words, the character of a spectrum of MCC

testifies to the removal of amorphous part of polymer and formation in its new crystal zones.

Thermogravimetric analysis (TGA), derivative thermogram (DTG) and differential scanning calorimetry (DSC) from temperature for MCC obtained from soybean straw under different liquor ration are presented in Fig. 4. The DSC signal was measured together with the TGA curve. The initial slight weight loss (almost 2–4 % to 120 °C) is due to evaporation and dehydration of adsorbed and surface water [36, 37]. Besides, the huge weight reduction began at 230 °C and ended at 340 °C, followed by slow weight loss up to 525–580 °C, which were attributed to the thermal degradation and complete degradation of cellulose and its conversion to char [37, 38]. According to [39, 40] the onset stage concerns the degradation, decarboxylation, depolymerisation and decomposition of glycosyl units in cellulose

is believed to be due to the evolution of non-combustible gases such as carbon dioxide, carbon monoxide, formic acid, and acetic acid while the second degradation stage is believed to be due to pyrolysis and evolution of combustible gases. It was observed that the residue remaining after degradation was 90 and 94 % for MCCs 10 and 15, respectively. This two-step process is also well reflected in the two DSC peaks shown in Fig. 4 *b* and two derived DTG peaks (Fig. 4 *a*). The TGA (Fig. 4 *a*) and DSC (Fig. 4 *b*) curves show that cellulose samples should not be heated above 220 °C. The peak decomposition temperature of the samples is visible on the derived weight loss curve (Fig. 4 *a*). The main peak decomposition temperature of MCCs is 327 and 313 °C for MCCs 10 and 15, respectively, which is in good agreement with the literature data [23, 32, 38].
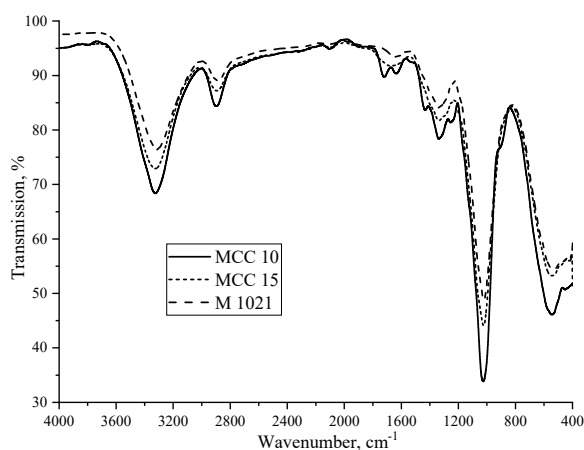

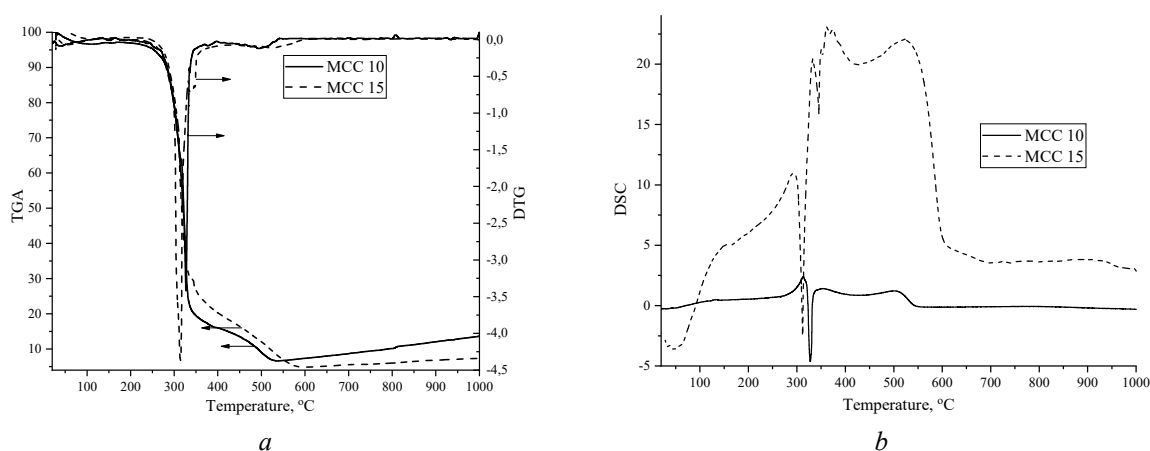**Fig. 3.** FT-IR spectra of obtained MCC compared to commercial M-1021

a   *b*

Fig. 4. TGA and DTG (*a*) and DSC (*b*) curves MCC isolated from soybean straw under different liquor ration

In Fig. 5 *a*, *b* the topography is shown of the MCC surface obtained from soybean straw under liquor ration 10. The surface shows clusters of individual particles, as well as elongated aggregates. These cross-sectional profiles indicate that the heights of the elements range from 23.8–28.1 nm (Fig. 5 *c*) to 16.9–26.8 nm (Fig. 5 *d*). Fig. 5 *e* shows a 2D image of a surface with a new cross-sectional line and profile. Analysis of the profile shows smaller heights compared to previous sections: 8.7, 9.1, 21.1, 5.3 nm (Fig. 5 *f*). In general, the particle sizes fit into the height range –17.5 + 45.5 nm, shown in the histogram (Fig. 5 *g*).
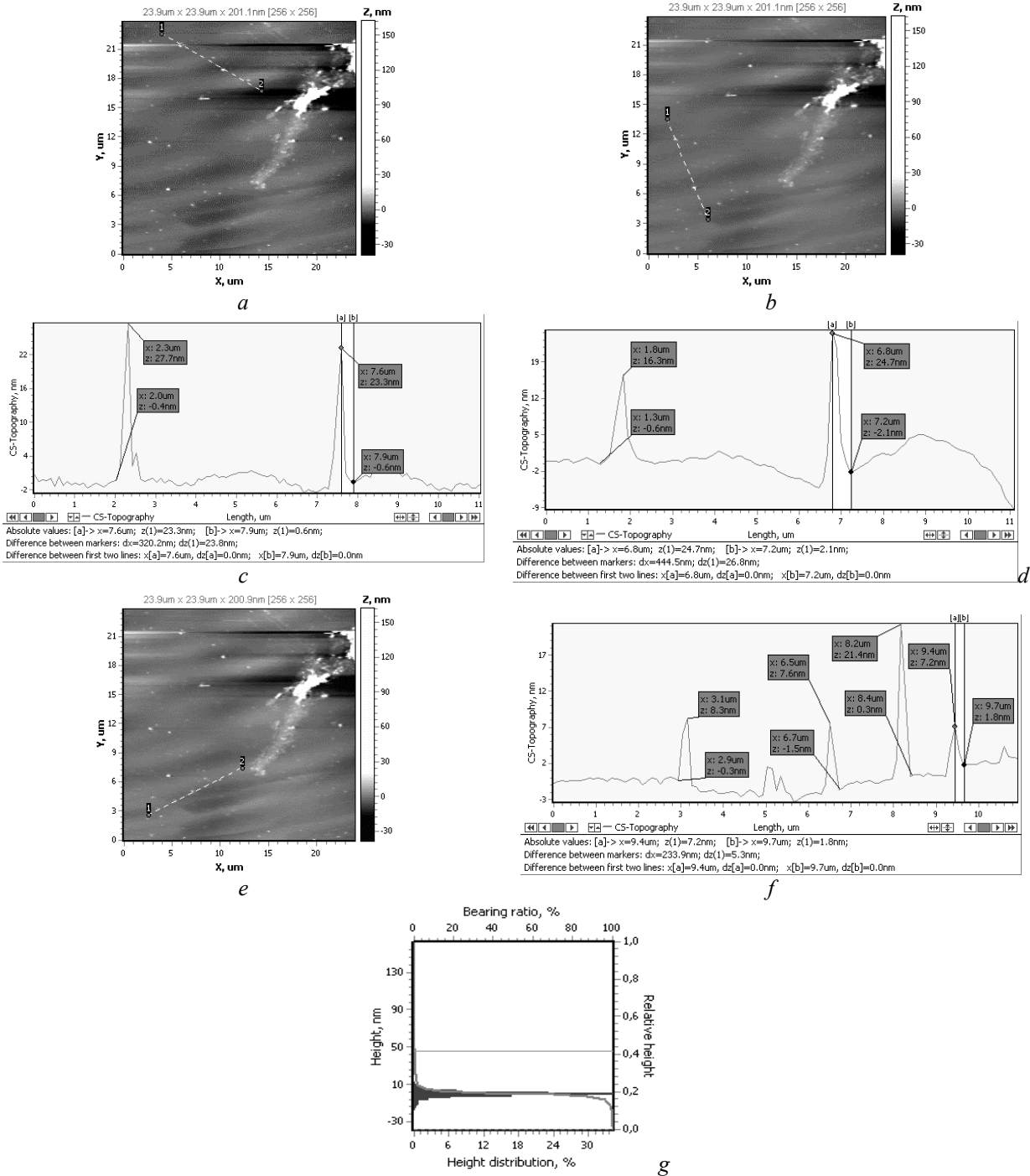

Fig. 5. 2D image of surfaces with shown cross-section lines (*a*, *b*, *e*), the profile of cross-section lines (*c*, *d*, *f*) and histogram of the distribution of depressions and heights on the 2D image (*g*)

It should be noted that when forming the surfaces of MCC particles, not only groups of particles are formed but also elongated aggregates, on the surface of which there are individual particles. This is clearly seen in 2D (Fig. 6 *a*) and 3D images (Fig. 6 *b*). The surface roughness is 1.6 nm. Fig. 6 *c* shows a 2D image with a cross-sectional line of an elongated aggregate, the analysis of the profile (Fig. 6 *d*) of which shows the nanosize of the particles.
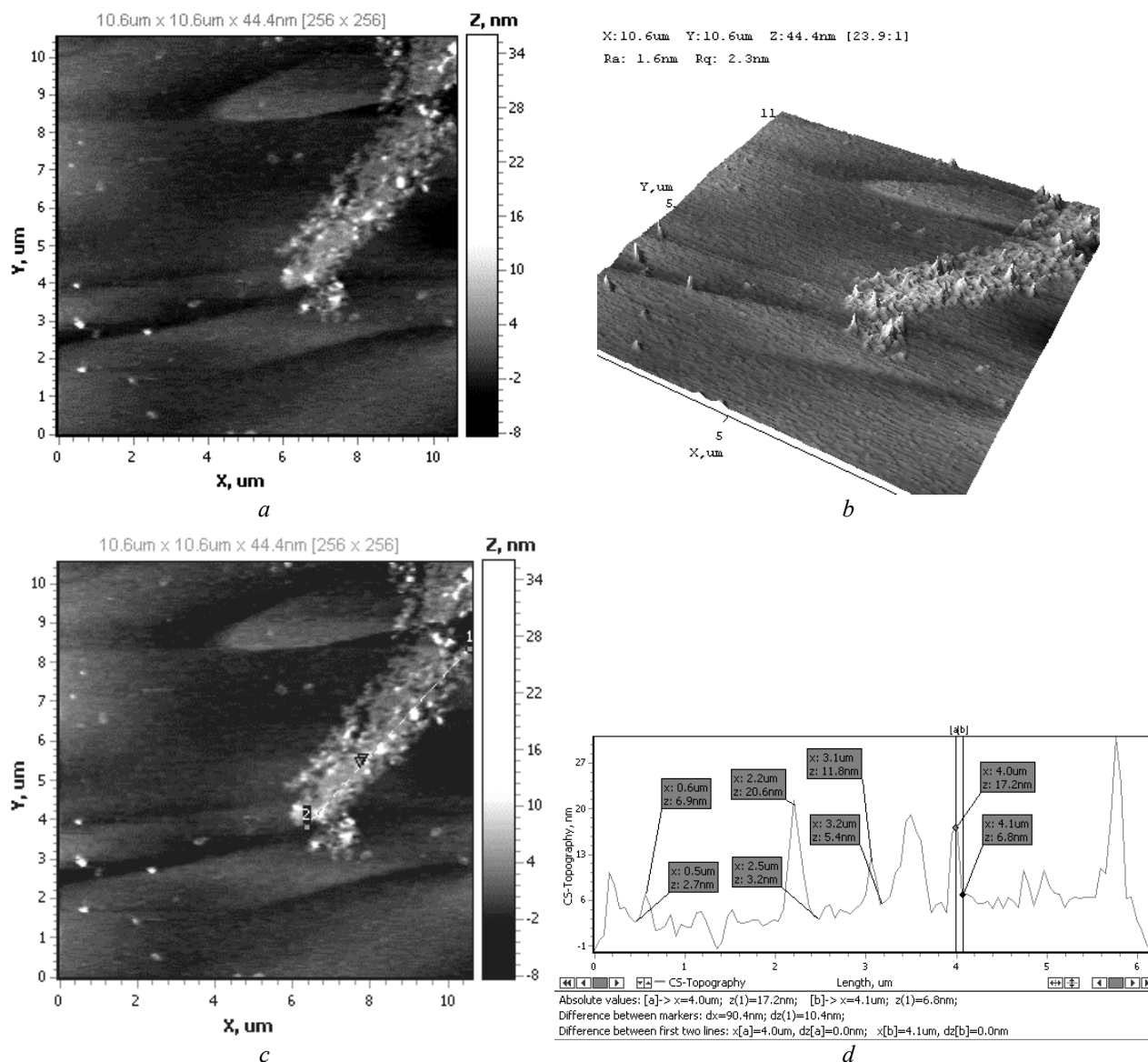
Fig. 6. 2D (*a*) and 3D (*b*) images of the surface with an elongated particle aggregate, 2D image with a cross-sectional line of the elongated aggregate (*c*) and profile (*d*)

Fig. 7 shows a 2D (*a*) and 3D (*b*) image of a surface with a selected fragment of a group of particles, as well as the fragment (*c*) with a sectional line along with the particles and their profile (*d*). The 3D image shows that the particles are pyramids with heights of 14.7–16.2 nm.

Fig. 8 shows the 2D (*a*) topography of the MCC surface obtained from soybean straw under liquor ration 15 and the 3D (*b*) image. The surface roughness is Ra = 3.1 nm. The particles are distributed throughout the scan, with no clusters of particles and their agglomerates. Analysis of the profiles of the cross-section lines drawn in different directions of the scan shows that the heights of the particles are 14.4, 18.7, 20.6, 17.4 nm (Fig. 8 *c, d*) and 23.9, 18.1, 24.7 nm (Fig. 8 *e, f*).

Fig. 9 shows the 2D (*a*) image with a selected fragment of distributed particles. In Fig. 9 c is the fragment itself and its 3D (*d*) image. The latter shows that the particles are pyramids of different configurations similar to the particles in MCC 10. The histogram of distribution of depressions and heights characteristic of this scan is shown in Fig. 9 *b*. It should be noted that the range of depressions and heights characteristic of MCC 15 is much smaller (from –13 to +20.7 nm) than in MCC 10 (from –17.5 to 45.5 nm) (Fig. 5).
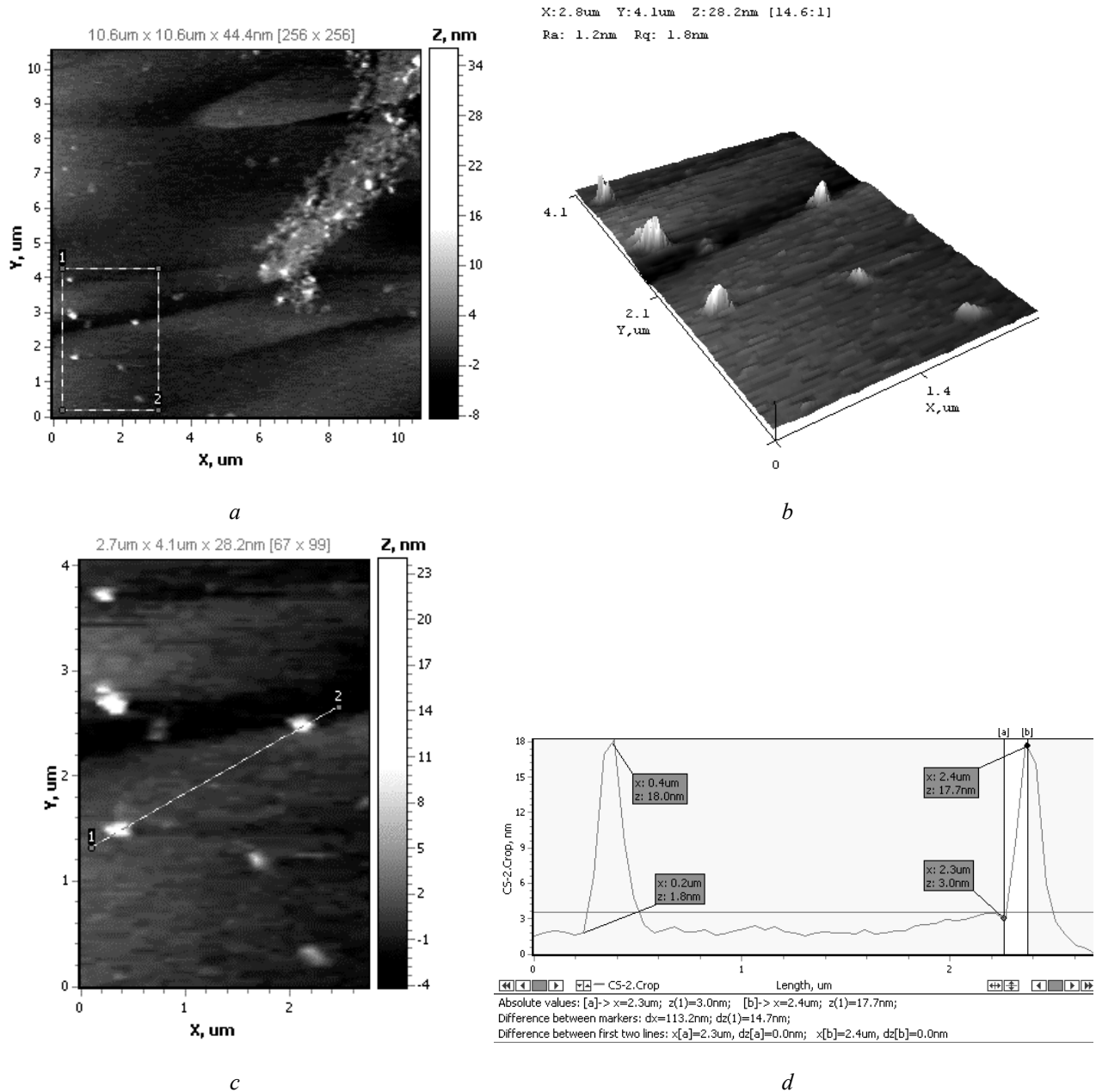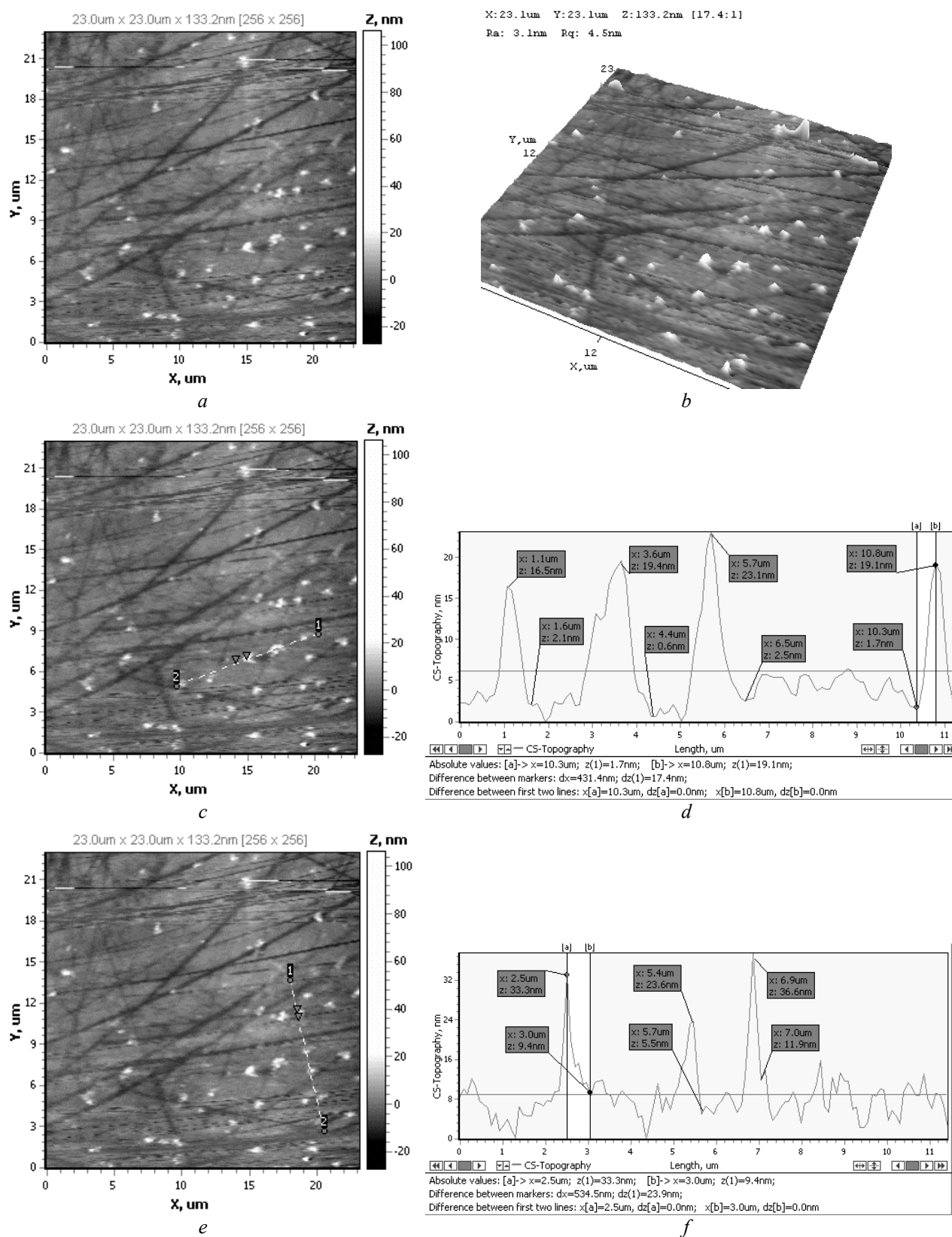

a



b

c

d

Fig. 7. 2D (*a*) and 3D (*b*) represent the surface with the selected fragment of the particle group, as well as fragment (*c*) with the line of intersection of the particles and its profile (*d*)

Fig. 8. Topography of 2D (*a*) surface of MCC obtained from soybean straw under liquor ration 15 and 3D image (*b*), the 2D image of the surface with cross-section lines in different directions (*c, e*) and profiles of their cross-section (*d, f*)
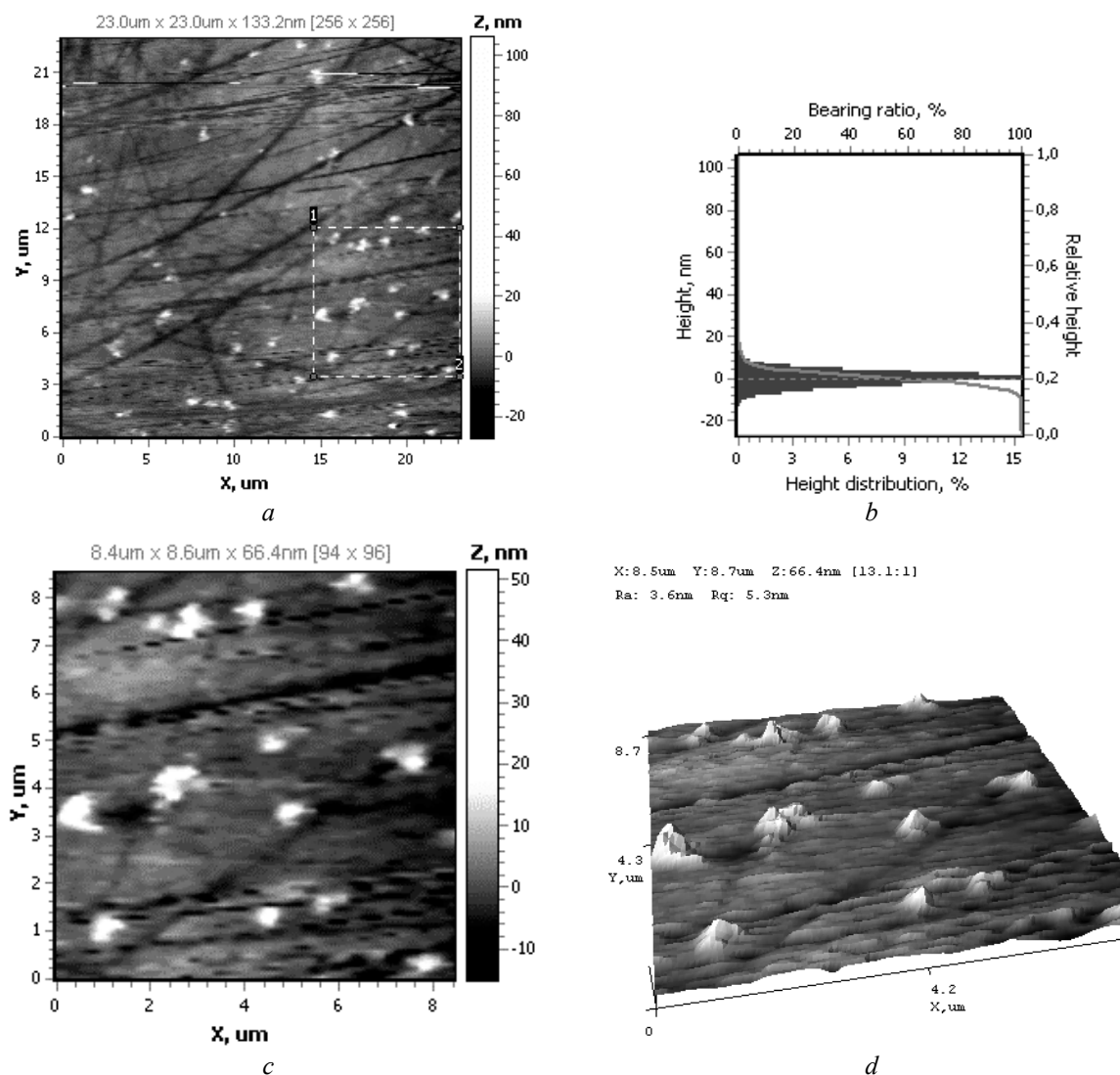
Fig. 9. 2D (*a*) image of the surface with the selected fragment of the group of particles, histogram of the distribution of depressions and heights (*b*) on the 2D image (–13 to +20.7 nm), the fragment (*c*) and its 3D image (*d*)

CONCLUSION

The influence of the liquor ratio on the physicochemical characteristics of the obtained microcrystalline cellulose was studied. It is found that increasing the hydromodule reduces the content of lignin and inorganic components. At the same time, both the MCC outputs and its qualitative characteristics are declining. First of all, as the liquor ration increases, the MCC crystallinity index decreases. The AFM method shows that when forming the surfaces of MCC 10 particles, not only groups of particles are formed but also elongated aggregates on the surface of which there are individual particles.

At the same time, the 3D image of the surface particles of MCC 15 shows that they are pyramids of different configurations similar to the particles in MCC 10. It should be noted that the range of depressions and heights characteristic of MCC 15 are much smaller than those of MCC 10.

ACKNOWLEDGEMENTS

Структурні та морфологічні особливості мікрокристалічної целюлози із соєвої соломи

Т.В. Ткаченко, Д.С. Каменських, Є.В. Шелудько, В.О. Євдокименко

Інститут біоорганічної хімії та нафтохімії імені В.П. Кухаря Національної академії наук України
вул. Мурманська, 1, Київ, 02094, Україна, ttv13ttv@gmail.com

Основною ідеєю даної роботи є дослідження можливості одержання мікрокристалічної целюлози з багатотонажного та малоцінного сільськогосподарського відходу та вивчення його структурних властивостей. Для дослідження використовувалась повітряно-суха соєва солома – відходи сільського господарства. З неї методом органо-сольвентної варки отримували мікрокристалічну целюлозу (МКЦ). За допомогою методів XRD, XRF, FTIR-ATR, AFM, TGA та DSC досліджено структуру та морфологію МКЦ. Встановлено, що збільшення гідромодуля знижує вміст лігніну та неорганічних компонентів. При цьому знижується як вихід МКЦ, так і її якісні характеристики. Перш за все, показник кристалічності МКЦ зменшується зі збільшенням кількості варильного розчину. У той же час смуга, що відповідала симетричним коливанням $-CH_2$ при 1435–1429 см$^{-1}$, яка відома як смуга кристалічності, зменшувалася зі збільшенням гідромодуля. Метод АСМ показує, що при формуванні поверхонь частинок МКЦ 10 утворюються не тільки групи частинок, висота елементів яких коливається від 23.8–28.1 до 16.9–26.8 нм, а й витягнуті одиниці, на поверхні яких є окремі частинки. Шорсткість поверхні 1.6 нм. У той же час поверхня МКЦ 15 має шорсткість Ra = 3.1 нм. Частинки розподілені по всій області сканування, без їхніх скупчень та агломератів, їхня висота 14.4, 18.7, 20.6, 17.4 і 23.9, 18.1, 24.7 нм. 3D-зображення частинок показало, що вони являють собою піраміди різної конфігурації, подібні до частинок у МКЦ 10. Діапазон западин і висот, характерних для МКЦ 15, значно менший (від –13 до +20.7 нм), ніж у МКЦ 10 (від –17.5 до 45.5 нм).

Ключові слова: мікрокристалічна целюлоза, соєва солома, гідромодуль, рельєф поверхні; атомно-силова мікроскопія

REFERENCES

1. Battista O.A., Smith P.A. Microcrystalline cellulose. *Ind. Eng. Chem*. 1962. **54**(9): 20.
2. FMC. Fun Facts about Avicel Microcrystalline Cellulose Also Known as Cellulose Gel. – 2013. Available from: http://www. fmcbiopolymer.com/Food/Home/News/FiftyYearso-fAvicel. aspx. (20.11.2021).
3. Albers J., Knop K., Kleinbudde P. Brand-to-brand and batch-to-batch uniformity of microcrystalline cellulose in direct tableting with a pneumo-hydraulic tablet press. *Pharmazeutische Industrie*. 2006. **68**(12): 1420.
4. Lee H.V., Hamid Sh.B.A., Zain S.Kh. Conversion of Lignocellulosic Biomass to Nanocellulose: Structure and Chemical Process. *The Scientific World Journal*. 2014. **2014**: 631013.
5. Luukkonen P. *Rheological properties and the state of water of microcrystalline cellulose and silicified microcrystalline cellulose wet masses*. (Diss Biocentri Viikki Univ Helsingiensis, 2001).
6. Jain J.K., Dixit V.K., Varma K.C. Preparation of microcrystalline cellulose from cereal straw and its evaluation as a tablet excipient. *Indian J. Pharm. Sci*. 1983. **45**: 83.
7. Paralikar K.M., Bhatawdekar S.P. Microcrystalline cellulose from bagasse pulp. *Biol. Wastes*. 1988. **24**(1): 75.
8. Uesu N.Y., Pineda F.A., Hechenleitner A.A. Microcrystalline cellulose from soybean husk effects of solvent treatments on its properties as acetyl-salicylic acid carrier. *Int. J. Pharm*. 2000. **206**(1–2): 85.
9. Bochek A.M., Shevchuk I.L., Lavrentev V.N. Fabrication of microcrystalline and powdered cellulose from short flax fiber and flax straw. *Russ. J. Appl. Chem*. 2003. **76**: 1679.
10. Alemdar A., Sain M. Biocomposites from wheat straw nanofibers: Morphology, thermal and mechanical properties. *Compos. Sci. Techol*. 2008. **68**(2): 557.
11. Bhattacharya D., Greminario L.T., Winter W.T. Isolation, preparation and characterization of cellulose microfibres from bagasse. *Carbohydr. Polym*. 2008. **73**(3): 371.
12. Cherian B.M., Leão A.L., de Souza S.F., Thomas S., Pothan L.A., Kottaisamy M. Isolation of nanocellulose from pineapple leaf fibres by steam explosion. *Carbohydr Polym*. 2010. **81**(3): 720.
13. Suesat J., Suwanruji P. Preparation and properties of microcrystalline cellulose from corn residues. *Adv. Mater. Res*. 2011. **332–334**: 1781.
14. Azubuike C.P., Okhamafe A.O. Physicochemical, spectroscopic and thermal properties of microcrystalline cellulose derived from corn cobs. *Int. J. Recyl Org. Waste Agric*. 2012. **1**: 1.

15. Oyeniyi Y.J., Itiola O.A. The physicochemical characteristic of microcrystalline cellulose, derived from sawdust, agricultural waste products. *Int. J. Pharm. Pharm. Sci.* 2012. **4**(1): 197.

16. Spigno G., Amendola D., Vellingiri V. Screening of four different agro-food by-products for the recovery of antioxidants and cellulose. *Chem. Eng. Transac.* 2014. **37**: 757.

17. Olugbenga O., Labunmi L., Bodunde O. Microcrystalline cellulose from plant wastes through sodium hydroxide-anthraquinone-ethanol pulping. *Bio. Res.* 2014. **9**(4): 6166.

18. Kuznetsov B.N., Taraban'ko V.E., Kuznetsova S.A. New catalytic methods for obtaining cellulose and other chemical products from vegetable biomass. *Kinet. Catal.* 2008. **49**(4): 517.

19. Barbash V.A., Yaschenko O.V., Shniruk O.M. Preparation and properties of nanocellulose from organosolv straw pulp. *Nanoscale Res. Lett.* 2017. **12**: 241.

20. Kuznetsov B.N., Chesnokov N.V., Garyntseva N.V., Yatsenkova O.V. Integrated catalytic processing of aspen wood into liquid and solid biofuels. *J. Siber. Fed. Univ. Chem.* 2013. **3**: 286.

21. Ejikeme P.M. Investigation of the physicochemical properties of microcrystalline cellulose from agricultural wastes I: orange mesocarp. *Cellulose.* 2008. **15**: 141.

22. Sherif S.Z. Hindi. Microcrystalline Cellulose: The Inexhaustible Treasure for Pharmaceutical Industry. *Nanosci. Nanotechnol. Res.* 2017. **4**(1): 17.

23. Kuthi F.A.A., Rabbi'atul N., Norzali'A., Badri Kh.H. Thermal characteristics of microcrystalline cellulose from oil palm biomass. *Malaysian Journal of Analytical Sciences.* 2016. **20**(5): 1112.

24. Tkachenko T.V., Yevdokymenko V.O., Kamenskyh D.S., Filonenko M.M., Vakhrin V.V., Kashkovsky V.I. Processing of vegetable waste of different origin. *Sci. Innov.* 2018. **14**(2): 48.

25. Tigunova O.O., Beiko N.E., Kamenskyh D.S., Tkachenko T.V., Yevdokymenko V.O., Kashkovskiy V.I., Shulga S.M. Lignocellulosic biomass after explosive autohydrolysis as substrate for butanol. *Biotechnologia Acta.* 2016. **9**(4): 28.

26. Obolenskaya A.V., Yelnitskaya Z.P., Leonovich A.A. *Laboratory work on the chemistry of wood and cellulose.* (Moscow: Ecology, 1991). [in Russian].

27. Swantomo D., Giyatmi, Adiguno S.H., Wongsawaeng D. Preparation of microcrystalline cellulose from waste cotton fabrics using gamma irradiation. *Eng. J.* 2017. **21**(2): 173.

28. Hu H., Zhang Y., Liu X., Huang Z., Chen Y., Yang M., Qin X., Feng Z. Structural changes and enhanced accessibility of natural cellulose pretreated by mechanical activation. *Polym Bull.* 2014. **71**: 453.

29. Herawan T., Panjaitan F.R., Yamanaka S. Morphological and structural changes in microcrystalline cellulose from OPEFB by mechanical grinding. In: *IOP conference series: earth and environmental science.* 2018. **166**: 012001.

30. Duan L., Yu W., Li Zh. Analysis of structural changes in jute fibers after peracetic acid treatment. *J. Eng. Fibers Fabr.* 2017. **12**(1): 33.

31. Tkachenko T., Sheludko Y., Yevdokymenko V., Kamenskyh D., Khimach N., Povazhny V., Aksylenko M., Kashkovsky V. Physico-chemical properties of flax microcrystalline cellulose. *Appl. Nanosci.* 2022. **12**: 1007.

32. Latif M.H.A., Mahmood Y.F. Isolation and Characterization of Microcrystalline Cellulose and Preparation of Nano-Crystalline Cellulose from Tropical Water Hyacinth. *Jour. for Pure & Appl. Sci.* 2018. **31**(1): 180.

33. Levdansky V.A., Levdansky A.V., Kuznetsov B.N. Ecology safe method of obtaining from firwood the cellulosic product with high content of alfa-cellulose. *Chemistry of Plant Raw Materials.* 2014. **2**: 35. [in Russian].

34. Hazwan Hussin M., Nurhanina Ayu Husin, Ibrahim Bello, Nurmaizatulhana Othman, Mohamad Abu Bakar, Mohamad Haafiz M.K. Isolation of Microcrystalline Cellulose (MCC) from Oil Palm Frond as Potential Natural Filler for PVA-LiClO$_4$ Polymer Electrolyte. *Int. J. Electrochem. Sci.* 2018. **13**: 3356.

35. Lokshina I., Lugovskoy S., Melisbekova K., Karabaev S.O., Gainullina I., Andreeva E. Microcrystalline cellulose: extraction and analysis. In: *Proceedings of the Fourteenth Israeli–Russian Bi-national Workshop.* (Ariel, 2015). P. 101.

36. Latif M.H.A., Mahmood Y.F. Isolation and characterization of microcrystalline cellulose and preparation of nano-crystalline cellulose from tropical water hyacinth. *J. Pure. Appl. Sci.* 2018. **31**(1): 180.

37. Jia N., Li S.-M., Ma M.-G., Zhu J.-F., Sun R.-C. Synthesis and characterization of cellulose-silica composite fiber in ethanol/water mixed solvents. *BioRes.* 2011. **6**(2): 1186.

38. Szczes´niak L., Rachocki A., Tritt-Goc J. Glass transition temperature and thermal decomposition of cellulose powder. *Cellulose.* 2008. **15**: 445.

39. El-Sakhawy M., Hassan M.L. Physical and mechanical properties of microcrystalline cellulose prepared from agricultural residues. *Carbohydr. Polym.* 2007. **67**(1): 1.

40. Trachea D., Hussinb M.H., Chuinb C.T.H., Sabarc S., Fazitad M.R.N., Taiwod O.F.A., Hassand T.M., Haafiz M.K.M. Microcrystalline cellulose: Isolation, characterization and bio-composites application. A review. *Int. J. Biol. Macromolecules.* 2016. **93**: 789.